

Fast Bayesian inference for slow-roll inflation

Christophe Ringeval*

*Centre for Cosmology, Particle Physics and Phenomenology
Institute of Mathematics and Physics, Louvain University
2 chemin du cyclotron, 1348 Louvain-la-Neuve, Belgium*

17 July 2018

ABSTRACT

We present and discuss a new approach increasing by orders of magnitude the speed of performing Bayesian inference and parameter estimation within the framework of slow-roll inflation. The method relies on the determination of an effective likelihood for inflation which is a function of the primordial amplitude of the scalar perturbations complemented with the necessary number of the so-called Hubble flow functions to reach the desired accuracy. Starting from any cosmological data set, the effective likelihood is obtained by marginalisation over the standard cosmological parameters, here viewed as “nuisance” from the early Universe point of view. As being low-dimensional, basic machine-learning algorithms can be trained to accurately reproduce its multidimensional shape and then be used as a proxy to perform fast Bayesian inference on the inflationary models. The robustness and accuracy of the method are illustrated using the Planck Cosmic Microwave Background (CMB) data to perform primordial parameter estimation for the large field models of inflation. In particular, marginalised over all possible reheating history, we find the power index of the potential to verify $p < 2.3$ at 95% of confidence.

Key words: cosmological parameters – cosmology:observations – early universe – inflation

1 INTRODUCTION

The recent release of the Planck CMB data (Ade et al. 2013e,f) and of the small scales CMB experiments (Hou et al. 2014; Dunkley et al. 2013; Sievers et al. 2013) have secured some generic predictions of inflationary cosmology: a very small spatial curvature today and an almost scale invariant primordial power spectrum for the cosmological perturbations. Ade et al. (2013c) reports a spectral index $n_s = 0.9603 \pm 0.0073$ using Planck temperature data complemented with WMAP polarization (Bennett et al. 2013; Hinshaw et al. 2013). Testing cosmic inflation is both a theoretical and experimental challenge. Originally, inflation was introduced to solve the problems of the standard Friedmann-Lemaître model of cosmology and this requires a period of accelerated expansion to take place in the early Universe (Starobinsky 1980; Guth 1981; Linde 1982; Albrecht & Steinhardt 1982). As such, inflation used to be referred to as a paradigm being difficult to test in itself as it could be implemented in various ways. However, getting the right spectrum for the cosmological perturbations requires the accelerated expansion to be complemented with some self-gravitating

scalar degree of freedom experiencing quantum fluctuations (Starobinsky 1979; Mukhanov & Chibisov 1981, 1982; Bardeen et al. 1983; Mukhanov 1985; Goncharov et al. 1987; Mukhanov 1988; Mukhanov et al. 1992). In its simplest implementation, such an evolution can be obtained with a single scalar field ϕ slowly rolling down a flat enough potential. These slow-roll models come with additional generic predictions, such as a small amount of non-Gaussianities and adiabatic initial conditions for the cosmological perturbations, both being in agreement with current cosmological data (Ade et al. 2013e,f). As discussed by Martin et al. (2014), the slow-roll class is already a populated landscape of well-motivated theoretical scenarios which make definite observable predictions. As such, testing single field inflation is challenging not because the models are too generic but because there are a very large number of different scenarios.

In this context, there are various ways to confront the slow-roll models with cosmological data. The basic approach consists in comparing crude predictions for the spectral index n_s and the tensor-to-scalar ratio r to existing bounds derived from a data analysis based on power law primordial power spectra. There are various issues with such an approach. First, the observable effects coming from the duration of the reheating era are omitted whereas, since the

* christophe.ringeval@uclouvain.be

WMAP data, those are known to be relevant for many models (Martin & Ringeval 2006, 2010). Secondly, predicting the spectral index, for a given inflationary model, usually relies on a first order expansion in a small parameter ϵ , proportional to the field velocity squared (in e -fold time), from which one can show that $n_s - 1 = \mathcal{O}(\epsilon)$. For a value of $n_s \simeq 0.96$, one has $\mathcal{O}(\epsilon^2) \simeq 2 \times 10^{-3}$ and one can question the relevance of the second order terms in view of the very small error bars on the current measurements on n_s (see above). Finally, let us stress that the true power spectra steaming from a given inflationary model do not generically have a power law shape. As such, one could also question the relevance of using (n_s, r) as a proxy to constrain the inflationary power spectra. Those questions used to be of negligible interest in a recent past as their effects were considered much smaller than the observational uncertainties. But as just argued, that is no longer the case with the Planck satellite results.

A way to alleviate these uncertainties is to numerically integrate the cosmological perturbations mode by mode during inflation (Salopek et al. 1989; Adams et al. 2001; Makarov 2005; Ringeval 2008). In that situation, for a given theoretical model, one obtains the exact primordial power spectra for both the tensor and scalar perturbations which depend on both the inflationary parameters $\{\theta_{\text{inf}}\}$ and the reheating parameters $\{\theta_{\text{reh}}\}$. For instance, considering a free massive scalar field of mass m to be the inflaton, the equations of motion for the perturbations in Fourier space involve both $\theta_{\text{inf}} = m$ and the wavenumber k . The reheating parameters $\{\theta_{\text{reh}}\}$ indirectly appear through the mapping between the physical wavenumbers observed today k/a_0 and the actual value of k/a during inflation. As a result, for any model of inflation, the power spectra have to depend on both $\{\theta_{\text{inf}}\}$ and $\{\theta_{\text{reh}}\}$. The method being exact, it is readily applicable to multifield inflation or more exotic models. Performing CMB data analysis from an exact numerical integration has been implemented for the first time by Ringeval et al. (2006); Martin & Ringeval (2006) and gives marginalised posterior distributions directly on to the fundamental parameters $\{\theta_{\text{inf}}, \theta_{\text{reh}}\}$ we are interested in. Moreover, the effects coming from the reheating being necessarily taken into account, this has been used to obtain the first CMB constraints on the reheating history in Martin & Ringeval (2010). Although now routinely used, see for instance Mortonson et al. (2011); Ade et al. (2013d), numerically integrating the inflationary spectra is computationally demanding. As a result, performing parameter estimation and Bayesian inference with this technique remains limited to a small number of models only (Martin et al. 2011; Easther & Peiris 2012).

In between, a precise way to perform CMB data analysis within slow-roll inflation has been discussed by Leach & Liddle (2003). It relies on the analytic expression of the primordial power spectra that can be consistently derived within the so-called slow-roll approximation (Mukhanov 1985; Stewart & Lyth 1993; Martin & Schwarz 2000; Schwarz et al. 2001; Leach et al. 2002; Schwarz & Terrero-Escalante 2004). Defining the Hubble flow functions (Hoffman & Turner 2001; Schwarz et al. 2001) (also named slow-roll parameters) by

$$\epsilon_{i+1} \equiv \frac{d \ln |\epsilon_i|}{dN}, \quad \epsilon_1 \equiv -\frac{d \ln H}{dN}, \quad (1)$$

with $H = \dot{a}/a$, $N \equiv \ln a$, a being the Friedmann-Lemaître-Robertson-Walker (FLRW) scale factor, one can check that the expansion of the Universe is accelerated when $\epsilon_1 < 1$ ($\ddot{a} > 0$). If the dynamics of the Universe is dominated by a scalar field, one can moreover show that $\epsilon_1 = (1/2)(d\phi/dN)^2$ (in Planck units), i.e. ϵ_1 is directly proportional to the field velocity squared. The slow-roll approximation assumes that all the $\epsilon_i \ll 1$ and are, at most, of the same order $\mathcal{O}(\epsilon)$. In that situation, the primordial power spectra can be derived analytically, at a given order in $\mathcal{O}(\epsilon)$. These calculations are non-trivial as they consist in solving the equations of motion for both the scalar and tensor perturbations during inflation. Currently, they have been completely performed up to second order (Stewart & Lyth 1993; Gong & Stewart 2001; Leach et al. 2002; Martin & Schwarz 2003; Habib et al. 2002, 2004; Casadio et al. 2005b,a; Lorenz et al. 2008b; Martin et al. 2013; Jimenez et al. 2013) and one obtains

$$\begin{aligned} \mathcal{P}_h = & \frac{2H_*^2}{\pi^2 M_{\text{P}}^2} \left\{ 1 - 2(1+C)\epsilon_{1*} + \left(\frac{\pi^2}{2} - 3 + 2C + 2C^2 \right) \epsilon_{1*}^2 \right. \\ & + \left(\frac{\pi^2}{12} - 2 - 2C - C^2 \right) \epsilon_{1*}\epsilon_{2*} + [-2\epsilon_{1*} + (2+4C)\epsilon_{1*}^2 \\ & \left. - 2(1+C)\epsilon_{1*}\epsilon_{2*} \right] \ln \left(\frac{k}{k_*} \right) + (2\epsilon_{1*}^2 - \epsilon_{1*}\epsilon_{2*}) \ln^2 \left(\frac{k}{k_*} \right) \Big\}, \end{aligned} \quad (2)$$

for the tensor modes and

$$\begin{aligned} \mathcal{P}_\zeta = & \frac{H_*^2}{8\pi^2 M_{\text{P}}^2 \epsilon_{1*}} \left\{ 1 - 2(1+C)\epsilon_{1*} - C\epsilon_{2*} \right. \\ & + \left(\frac{\pi^2}{2} - 3 + 2C + 2C^2 \right) \epsilon_{1*}^2 + \left(\frac{\pi^2}{24} - \frac{C^2}{2} \right) \epsilon_{2*}\epsilon_{3*} \\ & + \left(\frac{7\pi^2}{12} - 6 - C + C^2 \right) \epsilon_{1*}\epsilon_{2*} + \left(\frac{\pi^2}{8} - 1 + \frac{C^2}{2} \right) \epsilon_{2*}^2 \\ & + \left[-2\epsilon_{1*} - \epsilon_{2*} + (2+4C)\epsilon_{1*}^2 + (-1+2C)\epsilon_{1*}\epsilon_{2*} \right. \\ & \left. + C\epsilon_{2*}^2 - C\epsilon_{2*}\epsilon_{3*} \right] \ln \left(\frac{k}{k_*} \right) + \left(2\epsilon_{1*}^2 + \epsilon_{1*}\epsilon_{2*} + \frac{1}{2}\epsilon_{2*}^2 \right. \\ & \left. - \frac{1}{2}\epsilon_{2*}\epsilon_{3*} \right) \ln^2 \left(\frac{k}{k_*} \right) \Big\}, \end{aligned} \quad (3)$$

for the comoving curvature perturbation. In these expressions, all quantities with a “*” are functions evaluated at the conformal time η_* defined by

$$k_* \eta_* = -1, \quad (4)$$

i.e., the time at which a pivot mode of astrophysical interest today, for instance $k_* = 0.05 \text{ Mpc}^{-1}$, crossed the Hubble radius during inflation. The quantity $C = \gamma + \ln(2) - 2 \simeq -0.72964$, where γ is the Euler constant, stems from the integration of the equations of motion. These expressions are not exactly of a power law shape and show that performing inflationary data analysis using $\mathcal{P}_\zeta \propto (k/k_*)^{n_s-1}$ will necessarily introduce some bias of $\mathcal{O}(\epsilon^2)$.

Taking equations (2) and (3) as an input for cosmological data analysis consists in assuming that slow-roll inflation can be accurately described by the set of parameters $(H_*, \epsilon_{1*}, \epsilon_{2*}, \epsilon_{3*}, \dots)$. This is a fair assumption precisely because the Hubble flow hierarchy is constructed to do so, and any desired accuracy can be reached by including higher order terms. As an outcome, one obtains the marginalised probability distributions on H_* and the slow-roll param-

eters ϵ_{i*} (Leach & Liddle 2003; Martin & Ringeval 2006; Lorenz et al. 2008a; Finelli et al. 2010; Kuroyanagi et al. 2013). In fact, it turns out to be more convenient from a data analysis point of view to trade H_* for the quantity $P_* \equiv \mathcal{P}_c(k_*)$, i.e. the amplitude of the primordial anisotropies at the pivot scale. From equation (3), we see that H_* is indeed uniquely determined given $\{P_*, \epsilon_{i*}\}$.

Compared to an exact numerical integration, this is not really what we would like to obtain as the parameters we are interested in, for a given model of inflation, are $\{\theta_{\text{inf}}, \theta_{\text{reh}}\}$. However, once the potential is specified, the slow-roll approximation allows us to map, order by order, all the Hubble flow functions ϵ_i to the successive derivatives of the potential (Liddle et al. 1994). Therefore, within slow-roll, the functions $\epsilon_{i*}(\theta_{\text{inf}}, \theta_{\text{reh}})$ can be uniquely determined, as it is for the amplitude $P_*(\theta_{\text{inf}}, \theta_{\text{reh}})$. In fact, their analytic expressions for most of the single field models proposed so far can be found in Martin et al. (2014) and the associated public code ASPIC¹.

In this paper, we show that using equations (2) and (3) to extract an effective likelihood in the slow-roll variables space (P_*, ϵ_{i*}) , complemented by the knowledge of the functionals $\epsilon_{i*}(\theta_{\text{inf}}, \theta_{\text{reh}})$ and $P_*(\theta_{\text{inf}}, \theta_{\text{reh}})$, is enough to accurately constrain the inflationary parameters θ_{inf} and θ_{reh} of any slow-rolling inflationary model. Such an approach has the advantage of requiring only one complete analysis of the cosmological data sets under scrutiny, precisely to evaluate the effective likelihood, as opposed to one per model for an exact numerical integration. Moreover, the slow-roll approximation allows us to shortcut any mode integration and the determination of the actual values of $\epsilon_{i*}(\theta_{\text{inf}}, \theta_{\text{reh}})$ for any model consists in solving an algebraic equation for the reheating parameters. In section 2, we show how to practically implement this method using the publicly available codes COSMOMC (Lewis et al. 2000; Lewis & Bridle 2002) and MULTINEST (Feroz & Hobson 2008; Feroz et al. 2009; Trotta et al. 2008; Feroz et al. 2013), together with a basic machine-learning algorithm. Section 3 assesses its accuracy using the Planck 2013 data (Ade et al. 2013a) for the large field models of inflation. In particular, we show that there are no significant differences between the posterior distributions obtained from our approach and the posteriors steaming from a mode by mode exact integration of the inflationary perturbations pipelined with the exact likelihood provided by the Planck collaboration (Ade et al. 2013b). Finally, we conclude in section 4 and discuss how this approach could be generalized to any models of inflation.

2 METHOD

The first step consists in determining an effective likelihood in the inflationary parameter space. In the framework of Bayesian statistics, making inference on the parameters $\{\theta_{\text{inf}}\}$ and $\{\theta_{\text{reh}}\}$ is done by marginalisation over all the others, see for instance Trotta (2008). For CMB data, the marginalisation is therefore performed over the standard cosmological and astrophysical parameters, which are viewed as “nuisance” from the early Universe point of

view (Bridle et al. 2002). For instance, for a flat Λ Cold Dark Matter (Λ CDM) Universe, the standard cosmological parameters are $\{\theta_c\} = \{\Omega_b h^2, \Omega_{\text{dm}} h^2, \tau, \theta_{\text{MC}}\}$ where Ω_b is the density parameter of baryons, Ω_{dm} of cold dark matter, τ is the Thomson scattering optical depth, θ_{MC} encodes the angular size of the sound horizon at last scattering (Lewis & Bridle 2002) and h the reduced Hubble constant today. The marginalised posterior probability distribution for the primordial parameters $\{\theta_p\} \equiv \{\theta_{\text{inf}}, \theta_{\text{reh}}\}$, given some data set \mathbf{D} and some prior information I , reads

$$P(\theta_p | \mathbf{D}, I) = \int P(\theta_p, \theta_c, \epsilon | \mathbf{D}, I) d\epsilon d\theta_c, \quad (5)$$

where we have made explicit the standard cosmological parameters $\{\theta_c\}$ and have introduced a set of auxiliary parameters $\{\epsilon\} = \{\epsilon_0, \epsilon_1, \dots\}$. These auxiliary parameters allow us to extend the inference problem to the slow-roll parameter space, in a way similar to the introduction of hyperparameters (Hobson et al. 2002). For instance, we can choose to identify ϵ_0 to the scalar amplitude P_* and the ϵ_i to the Hubble flow hierarchy ϵ_{i*} . As discussed in the introduction, within a particular model of slow-roll inflation, the primordial amplitude and the slow-roll parameters are deterministic variables, i.e.

$$P(\epsilon | \theta_p, I) = \delta[\epsilon_0 - P_*(\theta_p)] \prod_{i \geq 1} \delta[\epsilon_i - \epsilon_{i*}(\theta_p)]. \quad (6)$$

From the Bayes’ theorem, the joint probability distribution in the right hand side of equation (5) can be expanded in

$$P(\theta_p, \theta_c, \epsilon | \mathbf{D}, I) = \frac{P(\theta_p, \theta_c, \epsilon | I) P(\mathbf{D} | \theta_p, \theta_c, \epsilon, I)}{P(\mathbf{D} | I)}. \quad (7)$$

Moreover, using the product rule and equation (6), one has

$$\begin{aligned} P(\theta_p, \theta_c, \epsilon | I) &= P(\theta_p, \theta_c | I) P(\epsilon | \theta_p, \theta_c, I) \\ &= P(\theta_p | I) P(\theta_c | I) \delta[\epsilon_0 - P_*(\theta_p)] \prod_i \delta[\epsilon_i - \epsilon_{i*}(\theta_p)], \end{aligned} \quad (8)$$

since $\{\theta_p\}$ and $\{\theta_c\}$ are independent parameter sets. Using these expressions, equation (5) simplifies to

$$P(\theta_p | \mathbf{D}, I) = \frac{\mathcal{L}_{\text{eff}}[\mathbf{D} | P_*(\theta_p), \epsilon_{i*}(\theta_p), I] P(\theta_p | I)}{P(\mathbf{D} | I)}, \quad (9)$$

where the marginalised effective likelihood is defined by

$$\mathcal{L}_{\text{eff}}(\mathbf{D} | P_*, \epsilon_{i*}, I) = \int P(\mathbf{D} | \theta_c, P_*, \epsilon_{i*}, I) P(\theta_c | I) d\theta_c. \quad (10)$$

Notice that the primordial parameters $\{\theta_p\}$ do no longer appear explicitly in the likelihood because, within the slow-roll approximation, the primordial power spectra are given by equations (2) and (3) such that the parameters that may affect the likelihood are $\{P_*, \epsilon_{i*}\}$ only. In some way, we are using the slow-roll functional shape of the primordial spectra to compress all of the available information into a minimal number of parameters.

In practice, one should first evaluate \mathcal{L}_{eff} by marginalisation of the full likelihood using equation (10). This requires a complete data analysis including the standard cosmological and astrophysical parameters, and can be computationally demanding, but this has to be done once and for all. Once \mathcal{L}_{eff} is determined, any slow-roll inflationary models can be dealt with equation (9). The dimension of the parameter

¹ <http://cp3.irmp.ucl.ac.be/~ringeval/aspic.html>

space being reduced, depending on how fast one can evaluate \mathcal{L}_{eff} , the speed of performing Bayesian inference and primordial parameter estimation can be significantly increased.

In the next section, we put these considerations into practice and use the Planck 2013 CMB data to determine \mathcal{L}_{eff} . Then, we apply our method to some typical inflationary models and compare the results to the ones coming from an exact numerical integration.

3 PRACTICAL IMPLEMENTATION

In order to determine \mathcal{L}_{eff} , we have first performed a complete CMB data analysis starting from the primordial power spectra given in equations (2) and (3), i.e. expanded at second order in the Hubble flow functions, that we now describe.

3.1 Slow-roll analysis of the Planck CMB data

The full likelihood $P(\mathbf{D}|P_*, \epsilon_{i*}, \boldsymbol{\theta}_c)$ is computed using the publicly available CLIK code provided by the Planck collaboration (Ade et al. 2013a,b). The Planck likelihood takes as an input the theoretical angular power spectrum of the CMB anisotropies, C_ℓ , for the polarization and the temperature, together with additional sets of astrophysical and observational parameters required to fit the foregrounds and various instrumental nuisances. In order to determine the C_ℓ given our cosmological and slow-roll parameters, we have used a modified version of the CAMB code (Lewis et al. 2000) to integrate the cosmological perturbations starting from the initial conditions given by our power spectra (2) and (3). More specifically, the underlying likelihood is the so-called CamSpec likelihood, described in Ade et al. (2013b), and the set of all cosmological, astrophysical and nuisance parameters is of dimension eighteen:

$$\{\boldsymbol{\theta}_c\} = \{\Omega_b h^2, \Omega_{\text{dm}} h^2, \tau, 100\theta_{\text{MC}}, \\ A_{100}^{\text{PS}}, A_{143}^{\text{PS}}, A_{217}^{\text{PS}}, r_{143 \times 217}^{\text{PS}}, A_{143}^{\text{CIB}}, A_{217}^{\text{CIB}}, r_{143 \times 217}^{\text{CIB}}, \\ \gamma^{\text{CIB}}, A_{\text{tSZ}}, A_{\text{kSZ}}, \xi^{\text{tSZ} \times \text{CIB}}, c_{100}, c_{217}, \beta_1^1\}. \quad (11)$$

The first four parameters have been described before and are the standard Λ CDM parameters. The next four respectively measure the power contribution at $\ell = 3000$ of unresolved point sources at 100 GHz, at 143 GHz, at 217 GHz and their cross correlation. The next three are their equivalent for the Cosmic Infrared Background (CIB), and γ^{CIB} stands for the spectral index of the CIB angular power spectrum. The next three parameters measure the unresolved Sunyaev-Zel'dovich contribution, thermal and kinetic and its correlation with the CIB. Finally, the last three parameters ensure marginalisation over calibration and beam uncertainties. More details on the modelling of all these signals can be found Ade et al. (2013b). In addition to the $\boldsymbol{\theta}_c$, our data analysis adds the four-dimensional set of slow-roll parameters $\{P_*, \epsilon_{1*}, \epsilon_{2*}, \epsilon_{3*}\}$.

Sampling the full parameter space has been performed with Markov chain Monte Carlo (MCMC) methods by using the publicly available COSMOMC code (Lewis & Bridle 2002), and under the same hypothesis described in Ade et al.

(2013c). In particular, our data sets are the Planck temperature measurements complemented by the WMAP polarization (Bennett et al. 2013), while all priors for the cosmological parameters $\{\boldsymbol{\theta}_c\}$ have been kept identical to those used by the Planck collaboration, see Table 4 in Ade et al. (2013c). Concerning the slow-roll parameters, we have chosen a Jeffreys' prior for the amplitude and for the first slow-roll parameter: $\ln(10^{10} P_*) \in [2.7, 3.4]$ and $\log(\epsilon_{1*}) \in [-5, 0]$. Indeed, the order of magnitude for those is a priori unknown. For the second and third slow-roll parameter, we have chosen a flat prior in $[-0.2, 0.2]$, motivated by the fact that both should be less than one. The MCMC exploration has been stopped according to the R-statistics convergence criteria implemented in COSMOMC (Lewis & Bridle 2002) and this merely requires the variance between mean values computed within each chain to be small enough. In our case, we have required it to be smaller than 0.001 and this amounts to keep a total number of samples around 2×10^6 . The marginalised posterior probability distributions for all the parameters have been plotted in figure 1. In the space of $\{\boldsymbol{\theta}_c\}$, we recover the same results as the Planck collaboration (Ade et al. 2013c). For completeness, we have also added the posteriors of the Hubble parameter H_0 and the cosmological constant Ω_Λ , which are derived from the ones we are sampling on. The slow-roll posteriors for $\{P_*, \epsilon_{1*}, \epsilon_{2*}, \epsilon_{3*}\}$ also match with those derived in Ade et al. (2013d), up to our prior which restrains ϵ_{3*} to small values in order to ensure the consistency of the slow-roll approximation. In order to make contact with the power law spectra analysis, let us notice that ϵ_{1*} is only bounded from above as it gives the tensor-to-scalar ratio $r = 16\epsilon_{1*} + \mathcal{O}(\epsilon^2)$ whereas ϵ_{2*} is well constrained because it carries most of the spectral index dependency $n_s = 1 - 2\epsilon_{1*} - \epsilon_{2*} + \mathcal{O}(\epsilon^2)$. On the other hand, one sees that ϵ_{3*} is not constrained, and exhibits at most a slight preference for positive values. This is also expected since it is linked to the running of the spectral index, which is not detected by Planck.

3.2 Effective likelihood

From equation (10), the effective likelihood \mathcal{L}_{eff} is simply the four-dimensional marginalised probability distribution in the (second order) slow-roll parameter space $\{P_*, \epsilon_{1*}, \epsilon_{2*}, \epsilon_{3*}\}$. It can be straightforwardly obtained from the previous CMB slow-roll analysis, while being more difficult to represent in a figure. At that point, one may nevertheless question the relevance of keeping ϵ_{3*} in \mathcal{L}_{eff} since this parameter remains unconstrained by the Planck data. In fact, nothing prevents us to marginalise equation (9) over any slow-roll parameter in addition to the cosmological ones. Doing so over ϵ_{3*} implies that the effective likelihood of equation (10) is now defined by marginalisation over $\{\boldsymbol{\theta}_c, \epsilon_{3*}\}$. Let us immediately stress that this is the correct Bayesian way to include any uncertainties coming from the unconstrained second order terms in the primordial power spectra, and that such an approach should become the standard lore to perform robust inference on the first order parameters.

From the previous discussion, we therefore consider a three-dimensional effective likelihood obtained by marginalising over all the $\{\boldsymbol{\theta}_c\}$ parameters of equation (11), plus ϵ_{3*} , thereby ending up with $\mathcal{L}_{\text{eff}}(\mathbf{D}|P_*, \epsilon_{1*}, \epsilon_{2*})$. Because this vo-

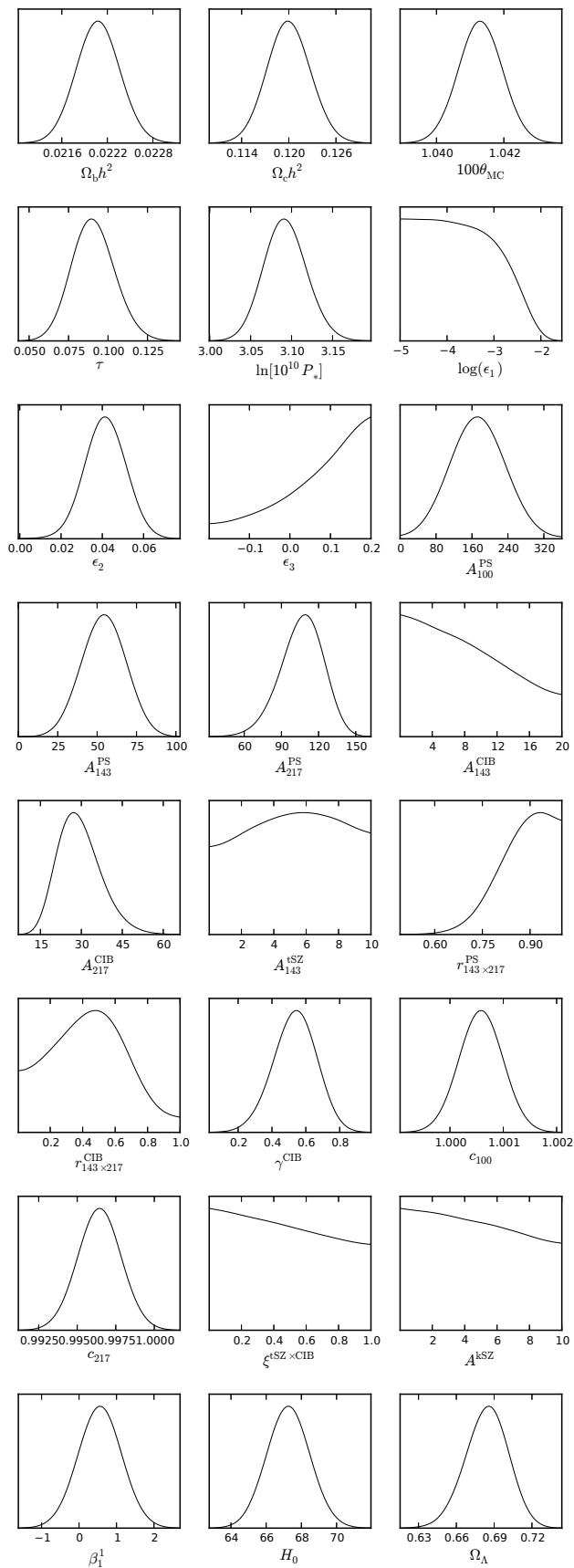


Figure 1. Marginalised posterior probability distribution for all the parameters associated with our CMB slow-roll analysis of the Planck 2013 data.

luminic function is at the basis of all our subsequent analysis, it has to be continuously defined for any values of its arguments. Being only known numerically, at a set of irregular discrete points obtained from the MCMC sampling, we have used basic machine-learning algorithms to numerically approximate its shape. In particular, we have tested both a radial basis function decomposition based on polyharmonic splines (Broomhead & Lowe 1988) and a more standard multivariate interpolation using a modified quadratic Shepard’s method (Shepard 1968; Thacker et al. 2010). The dimension remaining small, both methods were found to be accurate (see below) and fast: one evaluation of the likelihood requiring typically a few milliseconds on a standard laptop. An obvious limitation of this method comes from the finite number of samples obtained from the MCMC exploration: it is genuinely impossible to interpolate the likelihood in the regions in which it takes extremely low values. As one can guess, this is not very important because those regions have precisely no weight in the inference process. Typically, the lowest values for $\ln(\mathcal{L}_{\text{eff}}^{\text{min}}/\mathcal{L}_{\text{eff}}^{\text{max}}) = -10$ were obtained with the Shepard’s interpolation and this is the one we are considering in the following. In order to test the accuracy of the various numerical methods underlying the determination of \mathcal{L}_{eff} , we have re-derived from scratch the marginalised posterior distributions of the amplitude P_* and the slow-roll parameters ϵ_{1*} , ϵ_{2*} using only the machine-learned $\mathcal{L}_{\text{eff}}(\mathbf{D}|P_*, \epsilon_{1*}, \epsilon_{2*})$. In order to avoid any systematic, the slow-roll parameter space has been re-explored using the nested sampling algorithm implemented in the publicly available code MULTINEST (Feroz & Hobson 2008). In order to ensure a good convergence of the nested sampling, we have chosen the MULTINEST convergence criteria as in Feroz & Hobson (2008), i.e. a number of live points equals to 20000 and a target accuracy on the global likelihood (evidence) equals to 10^{-4} . In total, the nested sampling of \mathcal{L}_{eff} converged with a few hundred thousand samples in ten minutes on a standard laptop. The priors for the slow-roll parameters have been fixed as before (see section 3.1) and we have compared in figure 2 the one- and two-dimensional marginalised posterior distributions coming from both \mathcal{L}_{eff} and the previous full CMB analysis. As these plots emphasize, up to some very small deviations coming from the sampling uncertainties, there are no differences.

3.3 Parameter estimation for large field inflation

In the previous section, we have shown that our numerical implementation accurately reproduces the effective likelihood \mathcal{L}_{eff} in the slow-roll parameter space. We can now use it to perform parameter estimation within a given inflationary scenario and, as a proto-typical case, one can consider the “large field models”. These models are not currently favoured by the Planck data, but they have the advantage that everything can be worked out analytically thereby emphasizing the functional link between the slow-roll parameter space and the large field one. Moreover, precisely because they are not too close to the best fit region, these scenarios probe a region in our likelihood \mathcal{L}_{eff} which could be problematic. In other words, they constitute a good test case for the approach advocated here.

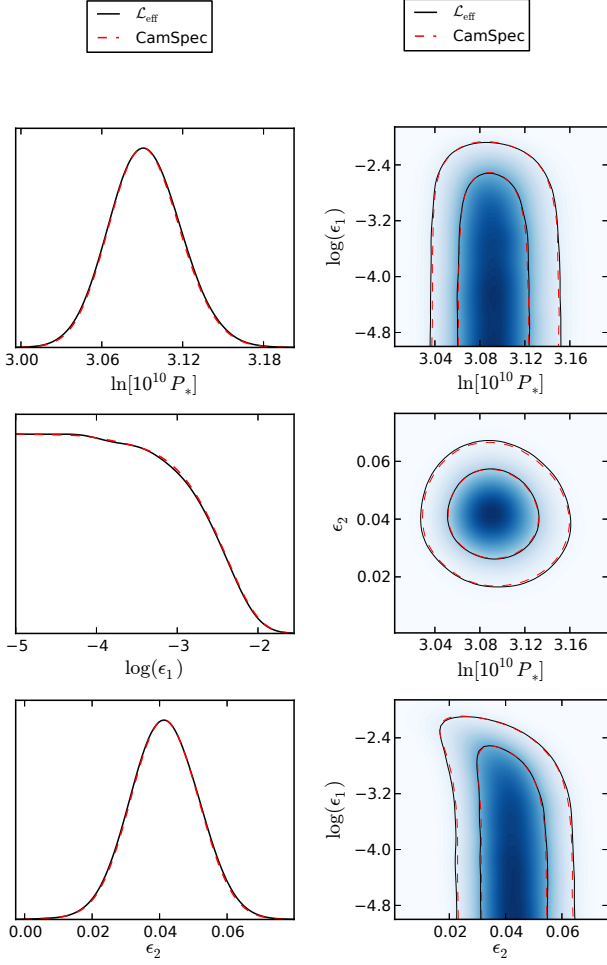


Figure 2. One and two-dimensional marginalised posteriors on P_* , ϵ_{1*} and ϵ_{2*} obtained from a complete MCMC exploration using the Planck likelihood (same as in figure 1) compared to the ones coming from nested sampling on our effective likelihood \mathcal{L}_{eff} . The differences are barely visible.

3.3.1 Reheating consistent slow-roll functionals

The large field potential is given by

$$V(\phi) = M^4 \left(\frac{\phi}{M_{\text{P}}} \right)^p, \quad (12)$$

and, within the slow-roll approximation, the first two Hubble flow functions read

$$\epsilon_1 = \frac{p^2}{2x^2}, \quad \epsilon_2 = \frac{2p}{x^2}, \quad (13)$$

where $x \equiv \phi/M_{\text{P}}$. The field evolution is obtained by solving the Friedmann-Lemaître and Klein-Gordon equations, again within the slow-roll approximation, and one obtains

$$N - N_{\text{end}} \simeq - \int_{x_{\text{end}}}^x \frac{V(x)}{V'(x)} dx = \frac{1}{2p} (x_{\text{end}}^2 - x^2). \quad (14)$$

As before, the quantity $N \equiv \ln a$ is the number of e -fold and x_{end} stands for the field values at which inflation ends. This equation can be inverted to give the field value x in terms of N as

$$x = \sqrt{x_{\text{end}}^2 - 2p(N - N_{\text{end}})}. \quad (15)$$

By definition, the end of inflation occurs at $\epsilon_1(x_{\text{end}}) = 1$, i.e. for

$$x_{\text{end}} = \frac{p}{\sqrt{2}}. \quad (16)$$

The only quantity that remains to be determined is x_* (or N_*), namely the field value at which the pivot mode k_* crossed the Hubble radius during inflation. Introducing the reheating parameter (Martin & Ringeval 2006, 2010; Martin et al. 2011; Ringeval et al. 2013)

$$R_{\text{rad}} \equiv \frac{a_{\text{end}}}{a_{\text{reh}}} \left(\frac{\rho_{\text{end}}}{\rho_{\text{reh}}} \right)^{1/4}, \quad (17)$$

one has

$$1 + z_{\text{end}} = \frac{1}{R_{\text{rad}}} \left(\frac{\rho_{\text{end}}}{\tilde{\rho}_\gamma} \right)^{1/4}. \quad (18)$$

The index “end” and “reh” denote the end of inflation and the end of the reheating era, respectively. The reheating parameter R_{rad} measures any deviations the expansion of the Universe may have during reheating compared to a pure radiation-like era. In the latter situation $R_{\text{rad}} = 1$ and the reheating era cannot be distinguished from the subsequent radiation dominated era. The quantity $\tilde{\rho}_\gamma \equiv \mathcal{Q}_{\text{reh}} \rho_\gamma$ is the energy density of radiation today eventually rescaled by $\mathcal{Q}_{\text{reh}} \equiv q_0^{4/3} g_{\text{reh}} / (q_{\text{reh}}^{4/3} g_0)$, the change of relativistic degrees of freedom between the reheating era and today. There, q and g respectively denote the number of entropic and energetic relativistic degrees of freedom. By definition of the pivot scale, one has

$$-k_* \eta_* \simeq \frac{k_*}{a(N_*)H(N_*)} = \frac{k_*}{a_0} \frac{a_0}{a_{\text{end}}} \frac{e^{N_{\text{end}} - N_*}}{H_*} = 1. \quad (19)$$

From equation (18), making use of the Friedmann-Lemaître equations, this expression can be recast into

$$\Delta N_* \equiv N_* - N_{\text{end}} = -\ln R_{\text{rad}} + \frac{1}{4} \ln \left[\frac{9}{\epsilon_{1*}(3 - \epsilon_{1\text{end}})} \frac{V_{\text{end}}}{V_*} \right] + N_0 - \frac{1}{4} \ln(8\pi^2 P_*) + \mathcal{O}(\epsilon), \quad (20)$$

in which $N_0 \equiv \ln[(k_*/a_0)/\tilde{\rho}_\gamma^{1/4}]$ roughly measures the number of e -folds of deceleration. We have now at our disposal all the equations needed to determine uniquely the observable slow-roll parameters. For any input of R_{rad} , one can solve the algebraic equations (20), using the potential (12) and the Hubble flow expressions (13) together with the trajectory (14). The solution gives x_* , or equivalently ΔN_* , from which one gets $\epsilon_{i*}(P_*, R_{\text{rad}}, p)$, i.e. the explicit functional relation linking the large field parameters to the slow-roll parameters.

In the previous equations, one can check that the potential parameter M cancels out. In fact, its dependency is implicit because it is in one-to-one correspondence with P_* . This can be seen from the first Friedmann-Lemaître equation, evaluated at $N = N_*$. In reduced Planck units ($M_{\text{P}} = 1$), defining $v_* \equiv V_*/M^4 = x_*^p$, one has

$$H_*^2 = \frac{V_*}{3 - \epsilon_{1*}} \simeq M^4 \frac{v_*}{3} + \mathcal{O}(\epsilon). \quad (21)$$

From the expression of the primordial power spectrum (3), $H_*^2 = P_*(8\pi^2 \epsilon_{1*}) + \mathcal{O}(\epsilon^2)$ and one finally gets

$$M^4 = 24\pi^2 \frac{\epsilon_{1*}}{v_*} P_* + \mathcal{O}(\epsilon^2). \quad (22)$$

Given P_* and x_* , this expression completely fixes the parameter M . In fact, it is more convenient to sample the parameter space using P_* instead of M because, as argued before, it is a well constrained quantity. In any case, one can always extract the posterior of M from the one of P_* by using equation (22).

Concerning the reheating, different choices are possible. One can sample directly on to the parameter R_{rad} introduced before, but, as can be seen in equation (20), R_{rad} exhibits some explicit dependence in P_* which will induce unnecessary correlations in the parameter space. Following Martin & Ringeval (2006), it is more convenient to sample on the rescaled reheating parameter R defined by

$$R \equiv R_{\text{rad}} \frac{\rho_{\text{end}}^{1/4}}{M_{\text{p}}}. \quad (23)$$

Plugging this expression into equation (20) yields, after some algebra with the Friedmann-Lemaître equations, a very similar expression (Martin & Ringeval 2010)

$$\Delta N_* = -\ln R + \frac{1}{2} \ln \left[\frac{9}{3 - \epsilon_{1\text{end}}} \frac{V_{\text{end}}}{V_*} \right] + N_0 + \mathcal{O}(\epsilon), \quad (24)$$

which does no longer depends on P_* (and with $\epsilon_{1\text{end}} = 1$ here).

From the previous considerations, we will define the large field inflationary parameter space to be

$$\theta_{\text{p}} = \{P_*, R, p\}. \quad (25)$$

3.3.2 Posteriors on the large field parameters from \mathcal{L}_{eff}

We have used MULTINEST to sample the parameter space of the large field models using the numerically approximated \mathcal{L}_{eff} discussed in section 3.2, together with the reheating consistent slow-roll expressions derived in the previous section. The convergence criteria have been chosen as before, namely 20000 live points and a target accuracy on the evidence equals to 10^{-4} (Feroz & Hobson 2008). The priors have been chosen flat on the power index $p \in [0.2, 5]$, with a Jeffreys' prior on $\ln(10^{10} P_*) \in [2.7, 3.4]$ and another Jeffreys' prior on the rescaled reheating parameter $\ln R \in [-46, 15]$. This last choice comes from the theoretical requirements of having the mean equation-of-state parameter during reheating $-1/3 < \bar{w}_{\text{reh}} < 1$, and by imposing to the reheating energy density $\rho_{\text{nuc}} < \rho_{\text{reh}} < M_{\text{p}}^4$. Here, $\rho_{\text{nuc}}^{1/4} \equiv 10 \text{ MeV}$ stands for the Big-Bang Nucleosynthesis energy scale. In addition to these priors, we have added a ‘‘hard prior’’ which enforces that $\rho_{\text{reh}} \leq \rho_{\text{end}}$ since the reheating era necessarily starts after the end of inflation. Those priors are discussed in more details in Martin & Ringeval (2010); Martin et al. (2011). In order to solve the algebraic equation (24), we have used the public code ASPIC which also computes the needed values of $\epsilon_{i*}(P_*, R, p)$. Convergence have been achieved with a few hundred thousand samples, and in about thirty minutes on a standard laptop. The one- and two-marginalised posteriors obtained from \mathcal{L}_{eff} have been plotted in figure 3. We recover that these models are under pressure, the power index p being constrained to be small. At 95% of confidence, we have $p < 2.3$ and $-37 < \ln R < 6$. These results suggest that, *marginalised over all possible reheating history*, massive inflation is still compatible with the Planck 2013 data.

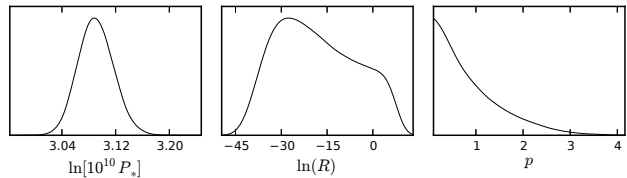


Figure 3. Marginalised posterior probability distributions obtained by nested sampling on \mathcal{L}_{eff} using the reheating consistent slow-roll functionals $\epsilon_{i*}(P_*, R, p)$ for large field inflation (ASPIC). One finds the power index $p < 2.3$ and the reheating parameter $-37 < \ln R < 6$, both at 95% of confidence.

3.4 Comparison with exact methods

The ultimate validation of the method is to compare the previous results to a CMB data analysis based on the exact Planck likelihood plus the exact primordial power spectra obtained by a mode-by-mode numerical integration of the perturbations during large field inflation. For this purpose, we have used the public code FieldInf² to integrate the scalar and tensor perturbations during inflation. The exact power spectra are then used within a modified version of the CAMB code which, coupled to COSMOMC and the CamSpec likelihood, allows us to perform a complete CMB data analysis within large field inflation.

For the primordial parameters P_* , $\ln R$ and p , the priors have been fixed exactly as in section 3.3.2 while the priors of all the other cosmological parameters have been chosen as in section 3.1. Such an analysis is in all point identical to the one performed by Martin & Ringeval (2010) using the WMAP seven years data (Larson et al. 2011; Jarosik et al. 2011). In particular, it is numerically quite demanding. Requiring the R -statistics convergence to be smaller than 5×10^{-3} has taken a few thousand hours of CPU-time on current x86-64 machines. In total, the posteriors plotted in figure 4 have been obtained from 500000 MCMC samples. In this figure, we have superimposed the posteriors of P_* , $\ln R$ and p coming from the fast analysis based on slow-roll and \mathcal{L}_{eff} (see figure 3). There is no difference, at least for P_* and the power index p . Only a hardly visible systematic up shift on the posterior of $\ln R$ seems to be present. If not due to differences between nested sampling and MCMC used for the fast and the exact method, respectively, it may come from some inaccuracies of the slow-roll approximation to determine x_{end} . Indeed, because solving $\epsilon_1(x_{\text{end}}) = 1$ is manifestly violating the slow-roll approximation, it is well known that equation (16) may induce some systematic errors of a few e -folds compared to the exact field trajectory. As a result, this translates into a systematic shift of the slow-roll approximated value of ρ_{end} , and as such, could affect $\ln R$. This could be easily improved, for instance by solving numerically the field value of x_{end} , although the bias induced on the posterior is, by far, of negligible importance with the current data. Let us notice that this concerns only models in which inflation ends at $\epsilon_{1\text{end}} = 1$, and not the model for which the reheating is triggered by a tachyonic instability ($\epsilon_{1\text{end}} \ll 1$ for those).

² <http://cp3.irmp.ucl.ac.be/~ringeval/fieldinf.html>

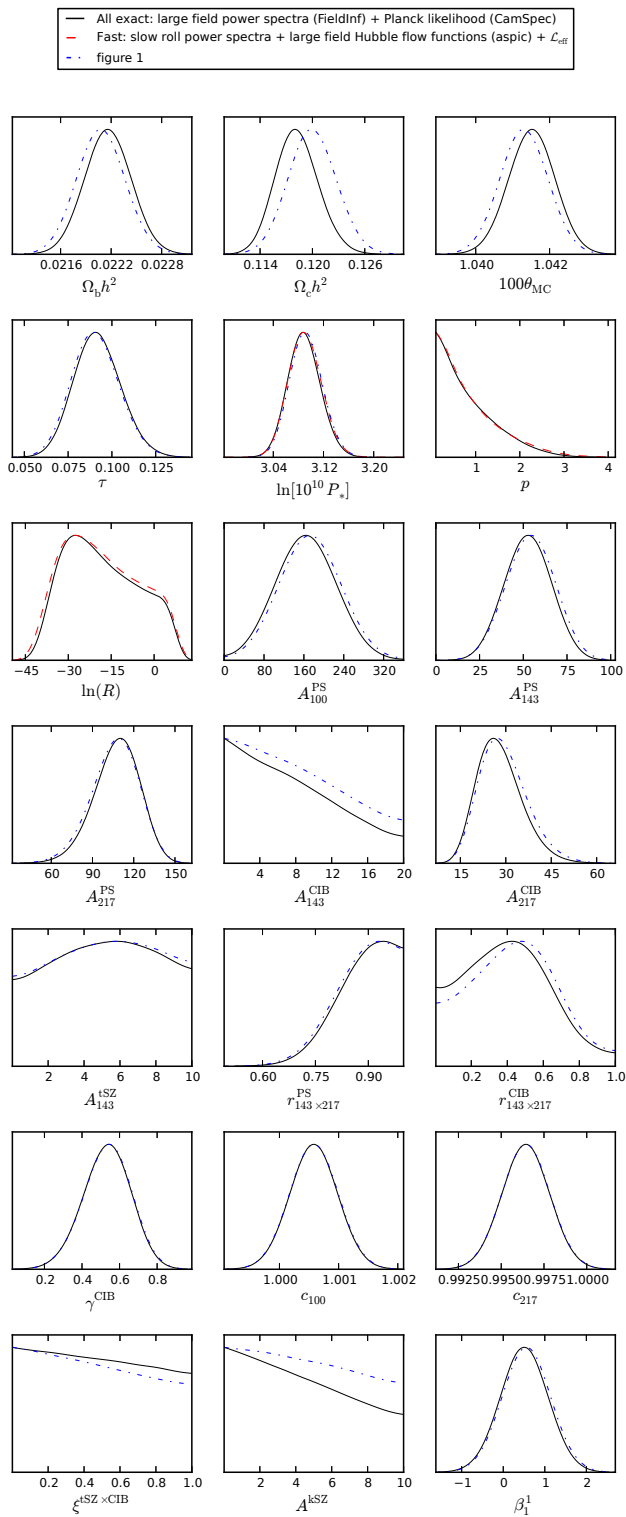


Figure 4. Marginalised posterior probability distributions for all the parameters associated with large field inflation. The solid black lines are obtained from the full Planck likelihood and the exact primordial power spectra obtained by a mode-by-mode integration using the `FieldInf` code. The posteriors of figure 3, stemming from the effective likelihood and approximate slow-roll relations, have been reported as red dashed lines for P_* , $\ln(R)$ and p . The agreement is excellent. For completeness, we have also reported the posteriors of the cosmological parameters found in figure 1 as blue dot-dashed lines. As expected, some of them differ due to the different primordial priors used (see text).

Marginalising over everything, we find the exact integration to give almost exactly the same two-sigma confidence intervals for the inflationary parameters. One gets $p < 2.2$ (instead of $p < 2.3$) and $-37 < \ln R < 6$ (unchanged) at 95% confidence. Interestingly enough, the upper limit on p is not better than the one coming from the WMAP data in Martin & Ringeval (2010). This may seem surprising at first, but, in the more usual language of power law power spectra, this can be traced back to a small shift in the best fit value of the spectral index n_s from WMAP to PLANCK. Notice that, on the contrary, the reheating parameter R is bounded from above by the Planck data while it was only limited from below by WMAP.

Let us finally stress that our method is dedicated to perform inference in the parameter space of inflation. As such, information on the standard cosmological parameters has been lost into the marginalisation process, but this is by choice because we were not interested in this issue here. For completeness, in figure 4, we have superimposed the posteriors of figure 1 for the $\{\theta_c\}$ parameters. The only difference between these posteriors come from the primordial power spectra: either they are second order slow-roll, or exactly integrated within large field inflation. Precisely because the large field models generically induce a too large tensor-to-scalar ratio, they badly fit the data and the most probable values for some of the cosmological parameters are accordingly shifted. Those effects cannot be studied within the above-described effective likelihood approach. One may nevertheless imagine to move one parameter, or more, from the set $\{\theta_c\}$ to the set $\{\theta_p\}$ in order to keep trace of them in the effective likelihood.

We conclude that using our effective likelihood for inflation, together with the slow-roll approximation, is accurate enough to deal with data sets as precise as those from the Planck satellite.

4 CONCLUSION

In this paper, we have presented a new method to perform inference on some primordial parameters $\{\theta_p\}$ associated with any model of slow-roll inflation. It relies on the determination of an effective likelihood \mathcal{L}_{eff} for inflation which is obtained by marginalisation over all the other parameters. This is summarized by equations (9) and (10). The effective likelihood being generically of much lower dimension, we have shown that it could be easily “machine-learned” thereby allowing for its fast numerical evaluation. Moreover, the low dimension of the problem also accelerates any Bayesian exploration of the primordial parameter space such that, in total, the speed-up reaches a few orders of magnitude compared to an exact method.

Here, we have used the slow-roll approximation to compress information on the primordial power spectra into a small set of parameters made of the primordial amplitude P_* and the Hubble flow functions ϵ_{i*} . For this reason, our approach can only be applied to the slow-rolling models of inflation precisely because they are accurately described by this approximation. As we have argued, even within this framework, the effective likelihood space could be extended to include any additional parameters we would like to per-

form inference on, eventually including some of the cosmological ones.

Let us also mention that integrating \mathcal{L}_{eff} over the parameters θ_p gives the global likelihood of any slow-roll models. In particular, this opens the window of fastly extracting and comparing the statistical evidences of all slow-roll inflationary models (Trotta 2007).

One may be worried that an effective likelihood for inflation can only be derived within slow-roll inflation. This is not the case. As long as one is able to determine a set of parameters modelling accurately the shape of the primordial power spectra, one can extract an effective likelihood over those parameters. In fact, we could readily extend our method to any model of inflation by binning the primordial power spectra over a given set of modes $\{\mathbf{k}\}$, and use some efficient machine-learning algorithms to fit its multidimensional shape, such as the recently released code SKYNET by Graff et al. (2012, 2013). From this, one could perform Bayesian inference on any inflationary models by using an exact integration code, such as `FieldInf`, to evaluate the power spectra bin per bin. Certainly this would not be as fast as using the slow-roll approximation, but by limiting the number of bins, the speed-up would still be significant.

Finally, although we have used the Planck data as a motivated test case, any cosmological data sets, or union of them, can be used in the definition of \mathcal{L}_{eff} . Equally, the approach is not limited to the power spectra and can be extended to other primordial observables, such as the bispectrum and trispectrum.

ACKNOWLEDGMENTS

It is a pleasure to thank J. Martin and V. Vennin for enlightening discussions. I would also like to thank the organisers and participants of the CosmoStats2013 conference where some ideas advocated here find their roots. This work is supported by the ESA Belgian Federal PRODEX Grant No. 4000103071 and the Wallonia-Brussels Federation Grant ARC No. 11/15-040.

REFERENCES

- Adams J. A., Cresswell B., Easther R., 2001, *Phys. Rev.*, D64, 123514, [arXiv:astro-ph/0102236](#)
- Ade P., et al., 2013a, [arXiv:1303.5062](#)
- Ade P., et al., 2013b, [arXiv:1303.5075](#)
- Ade P., et al., 2013c, [arXiv:1303.5076](#)
- Ade P., et al., 2013d, [arXiv:1303.5082](#)
- Ade P., et al., 2013e, [arXiv:1303.5084](#)
- Ade P., et al., 2013f, [arXiv:1303.5085](#)
- Albrecht A., Steinhardt P. J., 1982, *Phys. Rev. Lett.*, 48, 1220
- Bardeen J. M., Steinhardt P. J., Turner M. S., 1983, *Phys. Rev.*, D28, 679
- Bennett C., et al., 2013, *Astrophys.J.Suppl.*, 208, 20, [arXiv:1212.5225](#)
- Bridle S., Crittenden R., Melchiorri A., Hobson M., Kneissl R., et al., 2002, *Mon.Not.Roy.Astron.Soc.*, 335, 1193, [arXiv:astro-ph/0112114](#)
- Broomhead D., Lowe D., 1988, *Complex Systems*, 2, 321
- Casadio R., Finelli F., Luzzi M., Venturi G., 2005a, *Phys. Lett.*, B625, 1, [arXiv:gr-qc/0506043](#)
- Casadio R., Finelli F., Luzzi M., Venturi G., 2005b, *Phys. Rev.*, D72, 103516, [arXiv:gr-qc/0510103](#)
- Dunkley J., Calabrese E., Sievers J., Addison G., Battaglia N., et al., 2013, *JCAP*, 7, 25, [arXiv:1301.0776](#)
- Easther R., Peiris H. V., 2012, *Phys.Rev.*, D85, 103533, [arXiv:1112.0326](#)
- Feroz F., Hobson M., Cameron E., Pettitt A., 2013, [arXiv:1306.2144](#)
- Feroz F., Hobson M. P., 2008, *Mon. Not. R. Astron. Soc.*, 384, 449, [arXiv:0704.3704](#)
- Feroz F., Hobson M. P., Bridges M., 2009, *Mon. Not. R. Astron. Soc.*, 398, 1601, [arXiv:0809.3437](#)
- Finelli F., Hamann J., Leach S. M., Lesgourgues J., 2010, *JCAP*, 1004, 011, [arXiv:0912.0522](#)
- Goncharov A. S., Linde A. D., Mukhanov V. F., 1987, *Int. J. Mod. Phys.*, A2, 561
- Gong J.-O., Stewart E. D., 2001, *Phys. Lett.*, B510, 1, [arXiv:astro-ph/0101225](#)
- Graff P., Feroz F., Hobson M. P., Lasenby A., 2012, *Mon.Not.Roy.Astron.Soc.*, 421, 169, [arXiv:1110.2997](#)
- Graff P., Feroz F., Hobson M. P., Lasenby A. N., 2013, *Mon.Not.Roy.Astron.Soc.*, 441, 1741, [arXiv:1309.0790](#)
- Guth A. H., 1981, *Phys. Rev.*, D23, 347
- Habib S., Heinen A., Heitmann K., Jungman G., Molina-Paris C., 2004, *Phys. Rev.*, D70, 083507, [arXiv:astro-ph/0406134](#)
- Habib S., Heitmann K., Jungman G., Molina-Paris C., 2002, *Phys. Rev. Lett.*, 89, 281301, [arXiv:astro-ph/0208443](#)
- Hinshaw G., et al., 2013, *Astrophys.J.Suppl.*, 208, 19, [arXiv:1212.5226](#)
- Hobson M., Bridle S., Lahav O., 2002, *Mon.Not.Roy.Astron.Soc.*, 335, 377, [arXiv:astro-ph/0203259](#)
- Hoffman M. B., Turner M. S., 2001, *Phys.Rev.*, D64, 023506, [arXiv:astro-ph/0006321](#)
- Hou Z., Reichardt C., Story K., Follin B., Keisler R., et al., 2014, *Astrophys.J.*, 782, 74, [arXiv:1212.6267](#)
- Jarosik N., Bennett C., Dunkley J., Gold B., Greason M., et al., 2011, *Astrophys.J.Suppl.*, 192, 14, [arXiv:1001.4744](#)
- Jimenez J. B., Musso M., Ringeval C., 2013, *Phys.Rev.*, D88, 043524, [arXiv:1303.2788](#)
- Kuroyanagi S., Ringeval C., Takahashi T., 2013, *Phys.Rev.*, D87, 083502, [arXiv:1301.1778](#)
- Larson D., Dunkley J., Hinshaw G., Komatsu E., Nolte M., et al., 2011, *Astrophys.J.Suppl.*, 192, 16, [arXiv:1001.4635](#)
- Leach S. M., Liddle A. R., 2003, *Mon.Not.Roy.Astron.Soc.*, 341, 1151, [arXiv:astro-ph/0207213](#)
- Leach S. M., Liddle A. R., Martin J., Schwarz D. J., 2002, *Phys. Rev.*, D66, 023515, [arXiv:astro-ph/0202094](#)
- Lewis A., Bridle S., 2002, *Phys. Rev.*, D66, 103511, [arXiv:astro-ph/0205436](#)
- Lewis A., Challinor A., Lasenby A., 2000, *ApJ*, 538, 473, [arXiv:astro-ph/9911177](#)
- Liddle A. R., Parsons P., Barrow J. D., 1994, *Phys.Rev.*, D50, 7222, [arXiv:astro-ph/9408015](#)
- Linde A. D., 1982, *Phys. Lett.*, B108, 389
- Lorenz L., Martin J., Ringeval C., 2008a, *Phys.Rev.*, D78,

- 063543, [arXiv:0807.2414](#)
Lorenz L., Martin J., Ringeval C., 2008b, *Phys.Rev.*, D78, 083513, [arXiv:0807.3037](#)
Makarov A., 2005, *Phys. Rev.*, D72, 083517, [arXiv:astro-ph/0506326](#)
Martin J., Ringeval C., 2006, *JCAP*, 0608, 009, [arXiv:astro-ph/0605367](#)
Martin J., Ringeval C., 2010, *Phys.Rev.*, D82, 023511, [arXiv:1004.5525](#)
Martin J., Ringeval C., Trotta R., 2011, *Phys.Rev.*, D83, 063524, [arXiv:1009.4157](#)
Martin J., Ringeval C., Vennin V., 2013, *JCAP*, 1306, 021, [arXiv:1303.2120](#)
Martin J., Ringeval C., Vennin V., 2014, *Physics of the Dark Universe*, [arXiv:1303.3787](#)
Martin J., Schwarz D. J., 2000, *Phys. Rev.*, D62, 103520, [arXiv:astro-ph/9911225](#)
Martin J., Schwarz D. J., 2003, *Phys. Rev.*, D67, 083512, [arXiv:astro-ph/0210090](#)
Mortonson M. J., Peiris H. V., Easther R., 2011, *Phys.Rev.*, D83, 043505, [arXiv:1007.4205](#)
Mukhanov V. F., 1985, *JETP Lett.*, 41, 493
Mukhanov V. F., 1988, *Sov.Phys.JETP*, 67, 1297
Mukhanov V. F., Chibisov G., 1981, *JETP Lett.*, 33, 532
Mukhanov V. F., Chibisov G., 1982, *Sov. Phys. JETP*, 56, 258
Mukhanov V. F., Feldman H. A., Brandenberger R. H., 1992, *Phys. Rept.*, 215, 203
Ringeval C., 2008, *Lect. Notes Phys.*, 738, 243, [arXiv:astro-ph/0703486](#)
Ringeval C., Brax P., van de Bruck C., Davis A.-C., 2006, *Phys.Rev.*, D73, 064035, [arXiv:astro-ph/0509727](#)
Ringeval C., Suyama T., Yokoyama J., 2013, *JCAP*, 1309, 020, [arXiv:1302.6013](#)
Salopek D. S., Bond J. R., Bardeen J. M., 1989, *Phys. Rev.*, D40, 1753
Schwarz D. J., Terrero-Escalante C. A., 2004, *JCAP*, 0408, 003, [arXiv:hep-ph/0403129](#)
Schwarz D. J., Terrero-Escalante C. A., Garcia A. A., 2001, *Phys. Lett.*, B517, 243, [arXiv:astro-ph/0106020](#)
Shepard D., 1968, in *Proceedings of the 1968 23rd ACM national conference ACM '68*, A two-dimensional interpolation function for irregularly-spaced data. ACM, New York, NY, USA, pp 517–524
Sievers J. L., et al., 2013, *JCAP*, 1310, 060, [arXiv:1301.0824](#)
Starobinsky A. A., 1979, *JETP Lett.*, 30, 682
Starobinsky A. A., 1980, *Phys. Lett.*, B91, 99
Stewart E. D., Lyth D. H., 1993, *Phys. Lett.*, B302, 171, [arXiv:gr-qc/9302019](#)
Thacker W. I., Zhang J., Watson L. T., Birch J. B., Iyer M. A., Berry M. W., 2010, *ACM Trans. Math. Softw.*, 37, 34:1
Trotta R., 2007, *MNRAS*, 378, 72, [arXiv:astro-ph/0504022](#)
Trotta R., 2008, *Contemp. Phys.*, 49, 71, [arXiv:0803.4089](#)
Trotta R., Feroz F., Hobson M. P., Roszkowski L., Ruiz de Austri R., 2008, *JHEP*, 12, 024, [arXiv:0809.3792](#)